International Journal of
Scientific Engineering and Technology Research

ISSN 2319-8885
Vol.04,Issue.03
February-2015,
Pages:0547-0553

www.ijsetr.com

Half-Wave Cycloconverter Based PV Micro-inverter Topology Power Modulation with Phase Shift

PRASANNA KUMAR.CH[1], JAYAKRISHNA.G[2]
[1]PG Scholar, Dept of EEE, Narayana Engineering College, Gudur, AP, India.
[2]Professor &Head, Dept of EEE, Narayana Engineering College, Gudur, AP, India.

Abstract: In this paper, a grid-connected micro inverter with a less number of power conversion stages and fewer passive components is proposed. A high-frequency transformer and a series-resonant tank circuit is used to interface the full-bridge inverter to the half-wave cyclo-converter. All power switches are switched with zero voltage switching. Phase-shift power modulation is used to control the output power of the inverter. One of the first methods used to increase efficiency was to remove the high-frequency transformer at the input stage or the line frequency transformer at the output stage as in transformer less topologies. Unfortunately, transformer less topologies need more advanced control methods or modifications compared to existing topologies to keep dc current and leakage current injection in to the grid under control. Hence, there is an increased interest in grid isolated topologies as in with reduced number of power conversion stages, to increase the inverter efficiency and to reduce the number of passive components so as to increase the reliability of the system. In this paper a micro inverter with full-bridge inverter and a half-wave cycloconverter is proposed. Frequency modulation is used as the power control method of this inverter. There is only one power conversion stage and hence a reduced number of power switches resulting in reduced switching and conduction losses. The series-resonant tank is used to implement soft switching at the turn-on of the power switches to reduce switching losses due to the increased switching frequency. The proposed micro inverter is simulated using MATLAB/SIMULINK and the results are validated.

Keywords: Full-Bridge Inverter, Half-Wave Cycloconverter, Microinverter, Phase-Shift Power Modulation, Series-Resonant Circuit, Zero-Voltage Switching (ZVS).

I. INTRODUCTION

Renewable energy has become a hot research area as a result of increasing environmental issues due to fossil fuel combustion. Biomass, solar, wind, tidal, and geothermal are all potential renewable energy sources with low cost and reduced environmental effects. Solar energy plays a major role in renewable energy research as a sustainable and low environmental impact energy source. Among potential solar power generation systems, photovoltaic (PV) systems set to grow fastest. There are four major applications of PV power generation systems: off-grid domestic, off-grid non-domestic, grid connected distributed, and grid-connected centralized [1]. The PV inverter is the key element in grid-connected PV energy systems. The main functionality of the inverter is to convert PV-generated dc power into grid-synchronized ac output. Grid-connected PV inverters are categorized as micro-inverters, string inverters, multi-string inverters, mini central inverters, and central inverters according to the configuration of the inverter [2][3]. Among these inverter configurations, the microinverter has gained popularity, as it integrates a single solar panel (50–400 W) to the grid. Only a few years back, the cost of the overall inverter system was heavily dependent on the price of the PV module. With advancements in PV module manufacturing technology and with the quantity of production, the cost of the PV module has been drastically reduced. Presently, the cost of the PV system is highly dependent on the PV inverter topology.

Hence, new innovative topologies have been proposed [4]-[12] or PV micro inverters with the main purpose of increasing efficiency and reducing the manufacturing cost. Bringing down the count of power switches by reducing the number of conversion stages is one of the key strategies to address the efficiency of the system. Also, manufacturing cost of the system can be reduced by minimizing count and size of passive components and power switches. Importantly, as the lifetime of a modern solar panel is about 25 years [13], therefore guaranteeing the reliability of the micro-inverter throughout its lifetime has become essential. The main strategy used to increase the reliability of the system is the removal of the electrolytic capacitors from the system where possible, because the lifetime of electrolytic capacitors reduces with elevated temperatures [14]. Also, electrolytic capacitors contribute to the overall system cost in larger percentage. One of the first methods used to increase efficiency was to remove the high-frequency transformer at the input stage or the line frequency transformer at the output stage as in transformer-less topologies. Unfortunately, transformer-less topologies need more advanced control methods or modifications compared to existing topologies to keep dc current and leakage current injection into the grid under control[9],[10],[11]. Hence, there is an increased interest in grid isolated topologies as in with reduced number of power conversion stages, to increase the inverter efficiency and reduce the number of passive components so as to increase the reliability of the system[4]-[6].

A micro-inverter with full-bridge inverter and a half-wave cycloconverter is proposed in. Frequency modulation is used as the power control method of this inverter. Hence, it has some drawbacks such as a wide and unpredictable noise spectrum, more complex filtering of the output voltage ripple, and poor utilization of magnetic components [14]. A dual-active-bridge based micro-inverter with phase-shift modulation is proposed in [5]. Although there is a reduced number of power conversion stages as in [4], the number of power switches is increased compared to due to the four quadrant switches in the output side active bridge [4] as shown in Fig.1.

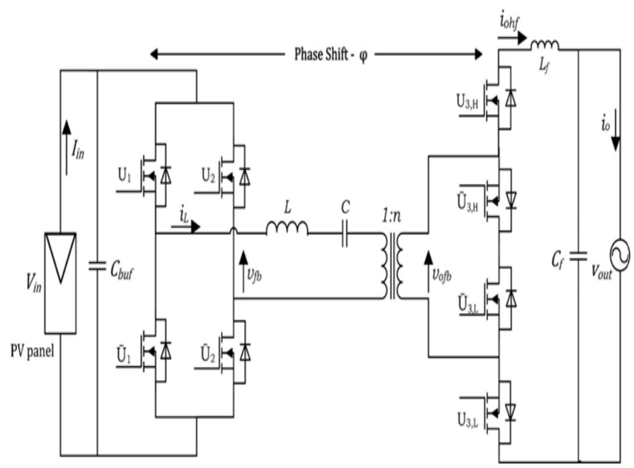

Fig. 1. Proposed microinverter topology.

II. TOPOLOGY DESCRIPTION

The full-bridge inverter is used as the primary-side inverter of the microinverter due to its higher voltage gain compared to the half-bridge inverter, although the number of switches in the full bridge circuit is twice that of the half-bridge. As a consequence, the turns ratio of the high-frequency transformer can be reduced by half, and hence, the size of the transformer can be reduced. A half-wave cycloconverter is used to integrate the microinverter to the grid at the secondary side. By using a half-wave cycloconverter, the number of switches in the secondary side can be reduced by half compared to a full-wave cycloconverter. This is expected to result in reduced switching and conduction losses in the overall inverter. In order to reduce the size of the isolation transformer, a higher switching frequency with a constant duty ratio (50%) is used to switch the power switches. As switching power loss in the active switches is proportional to the switching frequency, zero-voltage switching (ZVS) is used to turn ON all the switches in order to reduce turn-on switching losses. Turn-off switching power losses can be minimized by adding additional output capacitance to each power switch. ZVS is developed by using the resonant nature of the series-resonant tank current in the inverter.

The series-resonant tank can be placed either in the primary side, as shown in Fig.2, or in secondary side. Placement of the series-resonant tank in the secondary side may be more advantageous considering practical aspects, such as the number of turns needed in the secondary side is higher than that in the primary side with the same inductor core. The large number of turns allows the inductor to be wound in a more accurate manner. The resonant capacitor in the series-resonant tank can be used to block any dc voltage generated by the full bridge due to unbalanced operation. The passive filter capacitor C buff at the primary-side dc link is used to remove the double line frequency voltage and current ripple. The average size of that capacitor is in the milli farad range, and thus, electrolytic capacitors must be used as the filter. The size of the buffer capacitor can be reduced by using a series active buffer, as proposed in, or by using the third ripple port, as proposed in.

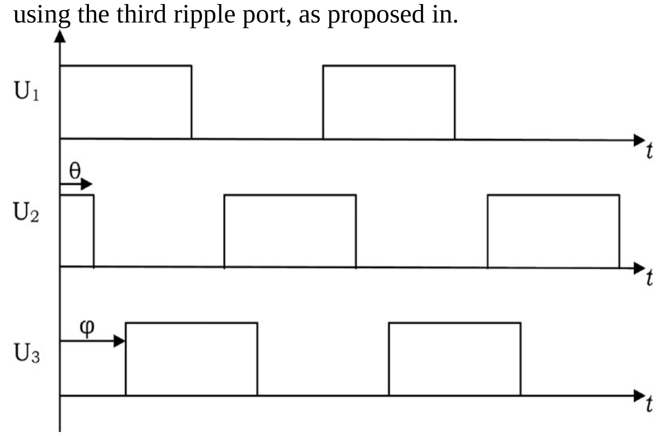

Fig.2. Switching signals of U_1, U_2, and U_3.

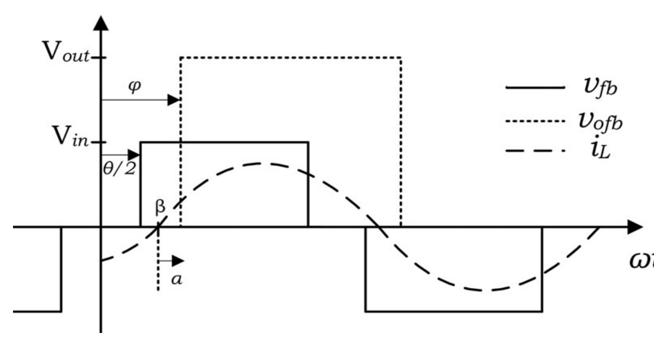

Fig.3. Waveforms of the full-bridge, half-wave cycloconverter and resonant current when $V_{out} > 0$.

The output filter capacitor C_f and inductor L_f in the secondary side are used to eliminate the switching frequency ripple in the output current.

A. Power Modulation

As two bridges are connected through the inductor, there are four power modulation methods, as given in and. Frequency modulation in the resonant circuit causes an unpredictable noise spectrum, resulting in more complex filtering of output voltage and poor utilization of magnetic components. Hence, phase-shift power modulation is used to control power output of this micro-inverter. All switches are switched using a constant f_s and a fixed duty ratio (50%). f_s is selected such that $f_s > f_r$, where f_r is the resonant frequency of the series resonant tank. Hence, the overall impedance seen by the full bridge is inductive and the resonant tank current will have a lagging power factor.

TABLE I: Switching Sequence of the Cycloconverter

		$u_{3,H}$	$\overline{u}_{3,H}$	$\overline{u}_{3,L}$	$u_{3,L}$
$\vartheta_{out}(+)\vartheta e$	$i_L(+)\vartheta e$	ON	OFF	OFF	ON
	$i_L(-)\vartheta e$	OFF	ON	ON	OFF
$\vartheta_{out}(-)\vartheta e$	$i_L(+)\vartheta e$	OFF	ON	ON	OFF
	$i_L(-)\vartheta e$	ON	OFF	OFF	ON

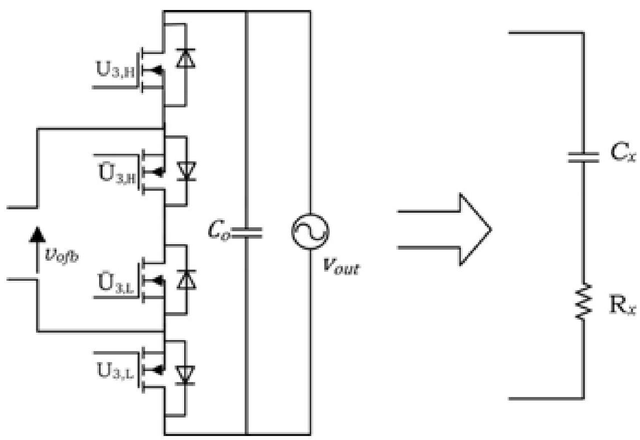

Fig. 4 Equivalent circuit of the half-wave cycloconverter.

The half-wave cycloconverter behaves as a controlled half-wave rectifier when α = 0◦. In such a case, the switching sequence of the half-wave cycloconverter is summarized in Table I. The grid-synchronized 50-Hz sinusoidal current can be obtained by varying the switching sequence starting instant with respect to the resonant current.

B. Power Flow Calculation

The ideal waveforms of the microinverter are shown in Fig. 3 by using two assumption made in Section II-A where PV input voltage and grid voltage are considered as constant over one switching period of the microinverter. The resonant current i_L of the inverter should lag the full-bridge output v_{fb} to ensure ZVS in the full-bridge inverter, as shown in Fig. Then, the anti parallel diode in the power switch will be turned ON before the power switch, ensuring there will be zero voltage across power switch when it turns ON. On the other hand, the resonant current should lead the cycloconverter input voltage v_{ofb}, in order to ensure ZVS in the half-wave cycloconverter. Also, ZVS turn-on of the cycloconverter depends on the switching sequence of the power switches. u3,L , u3,H should be completely turned ON when $V_{out} > 0$ and u3,H , ‾u3,L should be completely turned ON when $V_{out} < 0$ during each switching cycle in order to confirm ZVS in the cycloconverter switches. The cycloconverter can be represented by using an equivalent single reactive element, as shown in Fig. 4, due to the current lagging operation of the cycloconverter.

C. Soft-Switching Principle

A significantly higher switching frequency is used in the proposed inverter in order to reduce the size of passive components. However, switching power losses in the power switches are proportional to the switching frequency. ZVS is proposed as a soft-switching method for this inverter to reduce the switching power losses.

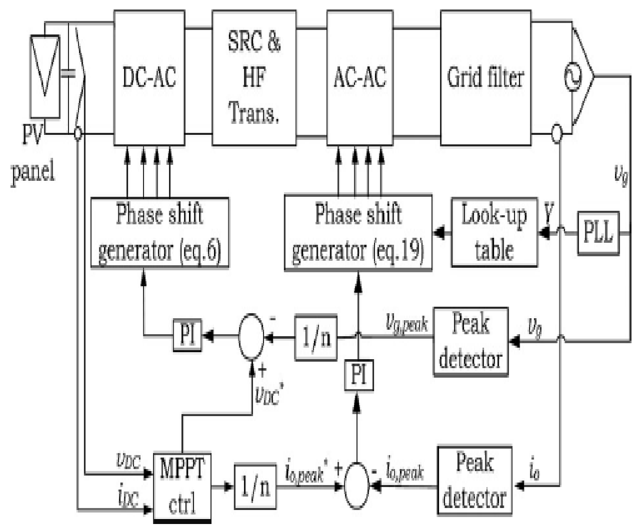

Fig. 5. Overall structure of the microinverter.

On the other hand, all power switches in the full-bridge are turned OFF with higher currents. Turn-off power losses in the switches can be minimized, adding additional output capacitance across each power switch.

D. Proposed Controller

The overall structure of the proposed microinverter is shown in Fig.5. The microinverter controller has two independent closed loops that control the output current (or power) and the PV-link voltage of the microinverter. The maximum power point (MPP) tracker locates and provides PV MPP voltage and current set point to the respective loop to obtain the desired control. In the current control loop, inverter phase shift ϕ is used to control the output current of the microinverter, as it can be shown from (19) that the current can be effectively regulated by controlling ϕ in the grid-connected mode. ϕ is varied within a specific limit based on the peak value of the grid current io and the reference grid current i∗ o, peak. The required ϕ is calculated by the phase-shift controller of the ac–ac converter, using the phase locked loop output γ as an input, as shown in Fig.5. The phase-shift controller can be developed either by using modulation methods or using a lookup table. Although the lookup table is proposed as a common ϕ control strategy for similar topologies, in this paper, the required output current is calculated by modulating ϕ using γ. The full-bridge phase shift θ can be used to control the PV-link voltage of the inverter according to (6) and, hence, the operating point of the PV characteristic curve. The MPP tracker output voltage v∗ DC is fed forward to generate a reference for the voltage control loop. All the constraints obtained in the Section II-D can be used to decide the allowable phase-shift combinations.

III. SIMULATION AND RESULTS

Firstly, simulations are done using passive networks for different positions of filter capacitors and inductors. For all the passive circuits, RLC load has been used and the position of the filter has been shuffled to observe the variations in the input and output voltages and currents and the amount of distortions present in them. Further, improvement of power factor is taken care of in the subsequent circuits where feedback loops are employed using analog circuits. A digital circuit implementation has also been carried out using UC3854 chip but it is observed that the power factor is very low. Hence, we are finally concerned with PFC using Analog circuits.

TABLE II: Microinverter Parameters

Parameter	Value
Resonant inductor (L)	$84.60\mu H$
Resonant capacitor (C)	120.9nF
Switching frequency (f_s)	$42.2kHz$
Quality factor (Q)	4
Input voltage (V_{in})	$40V$
RMS output voltage (v_{out})	$230V$
Transformer turns ratio (n)	8

The overall structure of the proposed microinverter is shown in Fig.6. The microinverter controller has two independent closed loops that control the output current (or power) and the PV-link voltage of the microinverter. The maximum power point (MPP) tracker locates and provides PV MPP voltage and current set point to the respective loop to obtain the desired control. In the current control loop, inverter phase shift ϕ is used to control the output current of the microinverter, as it can be shown from (19) that the current can be effectively regulated by controlling ϕ in the grid-connected mode. ϕ is varied within a specific limit based on the peak value of the grid current i_o and the reference grid current i_o, peak. The required ϕ is calculated by the phase-shift controller of the ac–ac converter, using the phase locked loop output γ as an input.

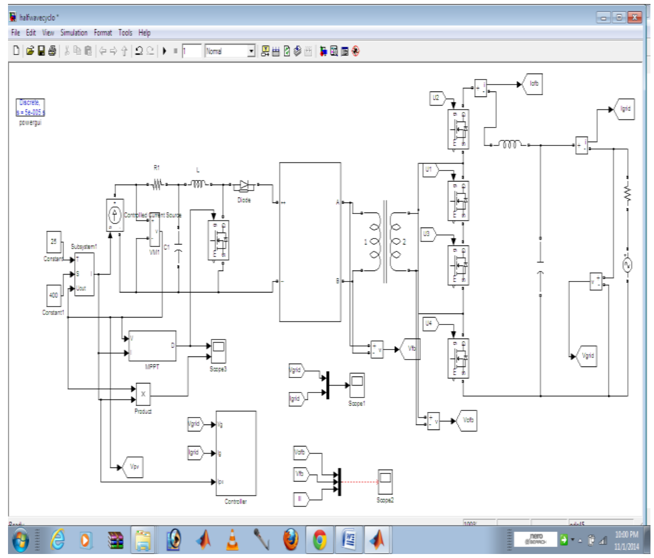

Fig.6. Main circuit of Half-Wave Cycloconverter-Based PV Microinverter.

The calculation of resonant components of the inverter is based on the equations presented in Section. With varying output power, it is difficult to choose the proper resonant component size to allow soft-switching operation throughout the whole operational range. Therefore, the average power of the inverter is used to calculate the equivalent load resistance of the inverter. The quality factor Q of the series resonant circuit is chosen as 4 in order to confirm validity of the sinusoidal approximation. The ratio of switching frequency to resonant frequency f is chosen as 1.1 in order to verify the soft-switching operation of all power switches of the inverter.

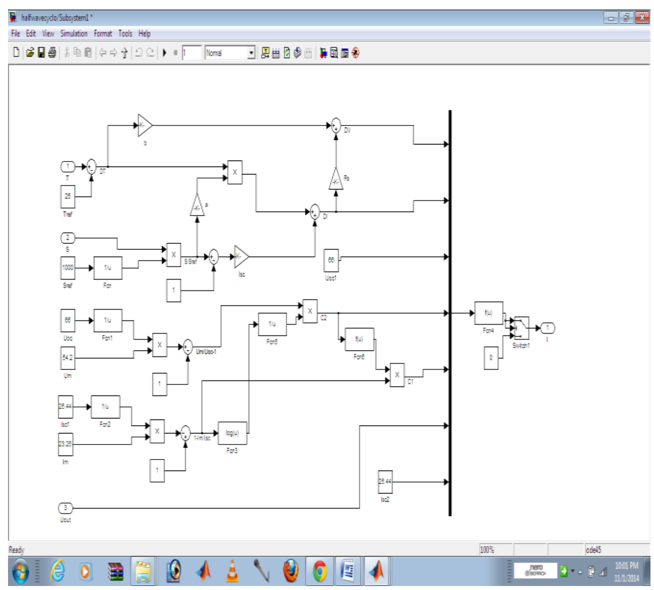

Fig.7. Half wave cycloconverter sub system.

Fig.7 shows in-phase grid voltage and current waveforms of the simulated microinverter rated to 278W and it is evident that used phase-shift modulation and its implementation is viable to use in this topology. Fig.8 shows the full-bridge output v_{fb}, the cycloconverter input v_{ofb}, and the primary-side resonant current i_L of the inverter at the positive peak of the grid voltage. The resonant current i_L lags the full-bridge output voltage v_{fb} and leads the cycloconverter input v_{ofb} and hence verifies that ZVS occurs at all power switches. unfiltered current i_{ohf} at the cycloconverter output. A similar set of waveforms is shown in at the negative peak of the grid voltage.

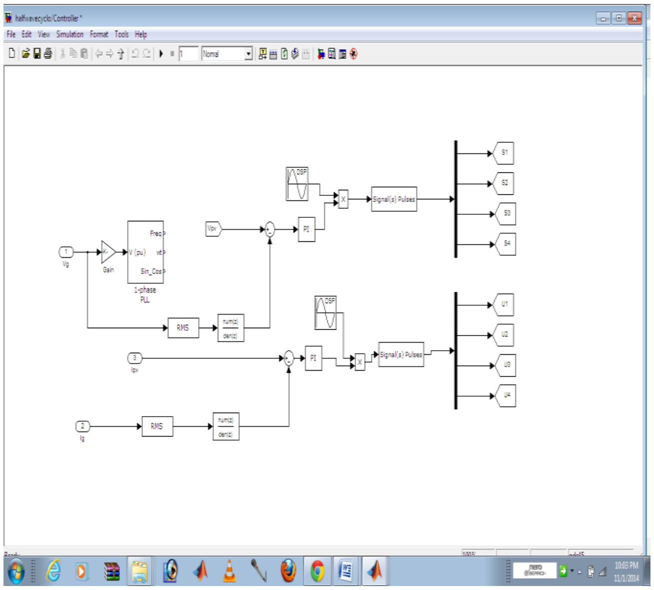

Fig.8. Controller circuit diagram.

The 100-W microinverter prototype is designed and built in the laboratory for verification purposes. Metal–oxide semiconductor field-effect transistors (MOSFETs) are used as power switches with appropriate voltage and current ratings. The MOSFET gate drivers are developed using opto-isolators and MOSFET gate drive integrated circuits (IC). A TMS320F28335 digital signal processor is used to control the microinverter. The dead bands in the input full-bridge control signals are chosen Full-bridge output voltage v_{fb} , resonant current i_L , and cycloconverter input voltage v_{ofb} at $\alpha = \pi^2$ in the positive half cycle of the inverter output.

TABLE III: Simulation Parameters

Parameter	Value
Resonant inductor (L)	$14.26\mu H$
Resonant capacitor (C)	$0.69\mu F$
Switching frequency (f_s)	$56.7kHz$
Leakage inductance of transformer primary winding	$0.1\mu H$
Leakage inductance of transformer secondary winding	$23.5\mu H$
Input voltage (V_{in})	$40V$
Transformer turns ratio (n)	8
Output filter capacitor (C_o)	$2\mu F$
Input buffer capacitor (C_{buf})	$8800\mu F$

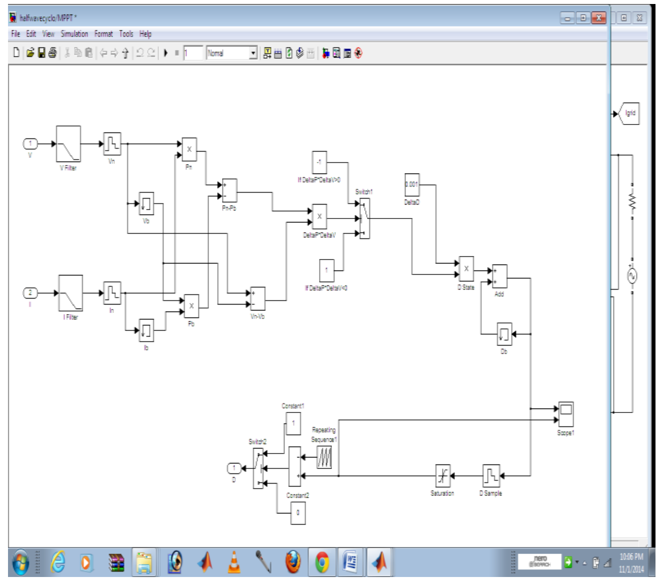

Fig.9. Mppt circuit diagram.

The maximum power point tracking (MPPT) capability of the microinverter is tested by using the same solar array simulator. The typical PV characteristic curves generated by the solar array simulator mode of the power supply are shown in Fig.9. The MPP tracker of the inverter is developed by using perturb and observation method (P&O). Peak power of the PV output curve is incremented in 2% intervals from the corresponding value of the lower curve of to the corresponding value of the upper curve in order to test the MPP tracking capability.

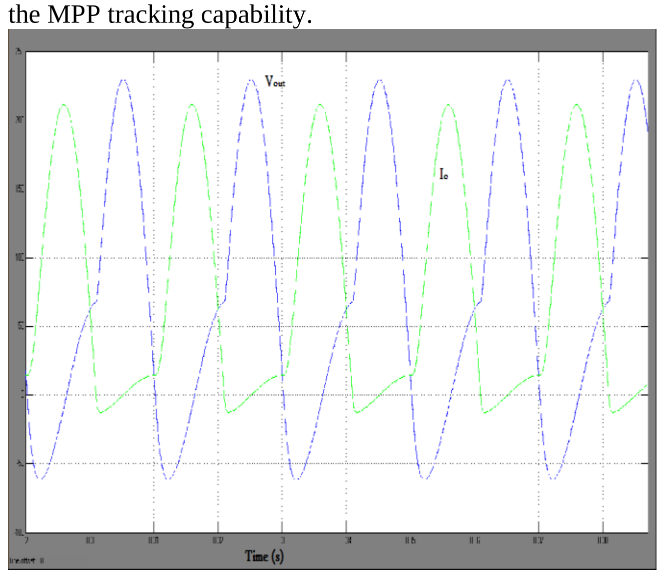

Fig.10. Output current(A)and grid voltage(V)of the inverter.

The results from that test are shown in Fig.11. In both modes, full-bridge phase shift θ is varied from its minimum to maximum value and inverter phase shift ϕ is varied from its minimum to maximum value at each step of θ which shows that the inverter is able to operate over a range of constant current and constant voltage points as well as at MPP of the tested PV curves.

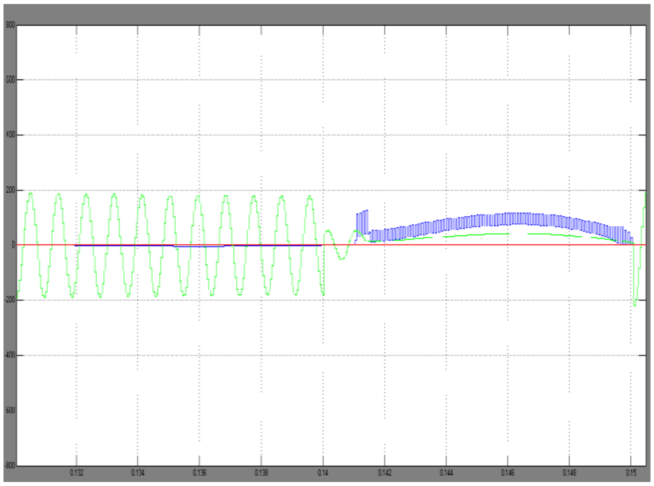

Fig.11. Simulated resonant current i_L ,full-bridge output voltage.

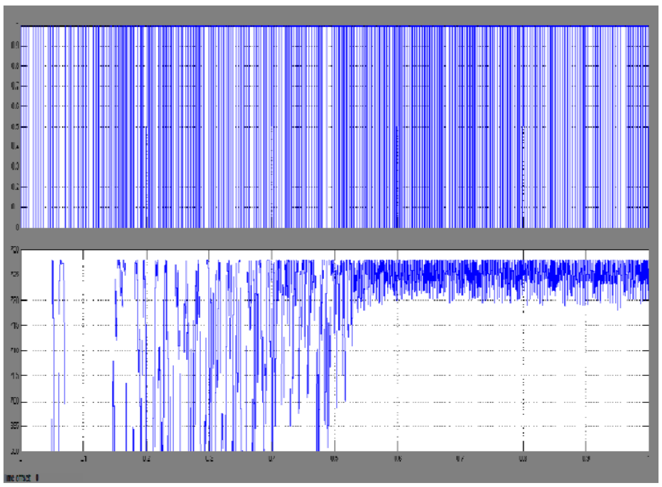

Fig.12. Simulated resonant current iL, full bridge output voltage (1:2) scaled cycloconverter input voltage.

A similar set of waveforms is shown in Fig at the negative peak of the grid voltage. Fig.12 shows that the full-bridge voltage v_{fb} leads the resonant current i_L and hence confirms the soft-switching operation at the input full-bridge. Also, the resonant current i_L leads the cycloconverter input, and hence, there is ZVS in the cycloconverter power switches.

IV. CONCLUSION

A microinverter topology is proposed with a half-wave cycloconverter and a full-bridge inverter. There is only one power conversion stage and hence a reduced number of power switches resulting in reduced switching and conduction losses. The transformer size is reduced because it is placed in the high-frequency link of the inverter resulting in a small and reduced weight system. The series-resonant tank is used to implement soft switching at the turn-on of the power switches to reduce switching losses due to the increased switching frequency. The operation of the inverter is critically analyzed and methods are presented to calculate the size of the resonant components. A relationship between the inverter phase shift, the full-bridge phase shift, the voltage gain of the inverter, the quality factor of the series-resonant tank, and the delivered power is derived. The soft-switching operation of the full-bridge and the half-wave cycloconverter is analyzed using the derived resonant current equation for the three stepped full-bridge output voltage and the half-wave cycloconverter input voltage. Simulation results are presented to verify the design process and the operation of the inverter. Therefore it is used as an efficient micro inverter in PV applications.

V. REFERENCES

[1] Philip C. Todd, "UC3854 Controlled Power Factor Correction Circuit Design", UNITRODE product and application handbook, 1995-1996.

[2] Laszlo Huber, Member IEEE, Liu Gang, and Milan M. Jovanovic, Fellow, IEEE, "Design Oriented Analysis and Performance Evaluation of Buck PFC Front End", 0885-8993/$26.00, 2010, IEEE.

[3] Huai Wei, IEEE Member, and Issa Batarseh, IEEE Senior Member, University of Central Florida, Orlando, FL 32816, " Comparison of Basic Converter Topologies for Power Factor Correction" , 0-7803-4391-3/98/$10.00 1998 IEEE.

[4] Muhammad H. Rashid, "Power Electronics Circuits Devices and Applications", Pearson Education, Inc., 2004.

[5] Vlad Grigore, " Topological Issues in Single Phase Power Factor Correction ", Dissertation for the degree of Doctor of Science in Technology, Helsinki University of Technology (Espoo, Finland) , 30th of November, 2001.

[6] Electrotek Concepts Inc. PQ Soft Case Study, "Power Factor Correction and Harmonic Control for dc Drive Loads", December 31, 2004.

[7] Smruti Ranjan Samal and Sanjay Kumar Dalai, "Power Factor Correction in a Single Phase AC-DC Converter", N.I.T. Rourkela, 2010.

[8] Temesi Erno, Michael Frisch, "PFC-Fundamentals, 2. Active Power Factor Correction – Principle of Operation", Tyco Electronics / Power Systems, Sept. 04

[9] P.C. Sen, "Thyristor DC Drives", Krieger Pub.Co.,1991.

[10] D. Cao, S. Jiang, and X. Yu, "Low-cost semi-z-source inverter for singlephase,"IEEE Trans. Power Electron., vol. 26, no. 12, pp. 3514–3523, Dec. 2011.

[11] L. Rossetto, Department of Electrical Engineering, G. Spiazzi & P. Tenti, Department of Electronics and Informatics, University of Padova, Via Gradenigo 6/a, 35131 Padova – Italy, 1994.

[12] K. Chomsuwan and P. Prisuwanna, "Photovoltaic grid-connected inverter using two-switch buck-boost converter," in Proc. IEEE Photovoltaic Spec. Conf., May 2002, pp. 1527–1530.

[13] F. Blaabjerg and Z. Chen, "Power electronics as efficient interface in dispersed power generation systems," IEEE Trans. Power Electron., vol. 19, no. 5, pp. 1184–1194, Sep. 2004.

[14] C. Rodriguez and G. Amaratunga, "Long-lifetime power inverter for photovoltaic AC modules," IEEE Trans. Ind. Electron., vol. 55, no. 7, pp. 2593–2601, Jul. 2008.

Author's Profile:

Ch.Prasanna Kumar received B.Tech degree in Electrical and Engineering from Quba Engineering College, nellore, in 2011. He is currently working towards M.Tech degree in Power Electronics in Narayana Engineering College, Gudur,A.P, India.

G.Jayakrishna received B.Tech, M.Tech and Ph.D degrees in Electrical Engineering from Jawaharlal Nehru Technological University, Anantapur, India in 1993,2004 and 2013 respectively. Currently he is working as professor & Head of Department of Electrical and Electronics Engineering, Narayana Engineering College, Gudur, A.P, India. His research interests include Power Quality, Electrical drives and Power Systems. He is life member of ISTE.